Cytofluorometric characterization of the myeloid compartment of irradiated mouse tumors

Marine Gerbé de Thoré, Lydia Meziani, Eric Deutsch, Michele Mondini

Version of Record: https://www.sciencedirect.com/science/article/pii/S0091679X22001297
Manuscript_c582f1457c7c03d37a274358a6e60454

Cytofluorometric characterization of the myeloid compartment of irradiated mouse tumors

Marine Gerbé De Thoré, Lydia Meziani, Eric Deutsch and Michele Mondini*

Gustave Roussy, INSERM U1030, Université Paris-Saclay, Villejuif, France.

*correspondence to Michele Mondini michele.mondini@gustaveroussy.fr and Eric Deutsch eric.deutsch@gustaveroussy.fr

Contents

Keywords: radiotherapy, myeloid cells, flow cytometry, immune system, head and neck cancer

Abstract

The use of ionizing radiation (IR) is a cornerstone for the treatment of cancer and radiotherapy (RT) is used in roughly 50% of cancer patients. It is now well established that RT exerts widespread effects on the tumor stroma, including the immune environment. Together with its deeply characterized effects on the lymphoid compartment, RT also deeply affects the myeloid cell compartment. Fluorescence-activated flow cytometry is one of the most widely used technologies in immunology, allowing the multiparametric analysis of cells on a cell-by-cell basis. Here, we provide a detailed flow cytometry protocol to analyze the myeloid cell populations of human papillomavirus (HPV)-positive TC1/Luc tumors engrafted in the oral mucosa of immunocompetent mice, and to evaluate their modulations in response to RT. The same method, with slight modifications, can be used to study the tumor myeloid cells from a variety of other mouse tumors.

1. Introduction

Radiotherapy (RT) is a mainstay for cancer therapy and contributes to the treatment of more than 50% of all cancer patients (Baskar et al., 2012; Baumann et al., 2020), including a significant proportion of head and neck squamous cell carcinoma cancer. Together with RT cytotoxic activity, evidence accumulated concerning the involvement of the immune system in mediating its therapeutic efficacy (Mondini et al., 2020). Indeed, especially in the last

decade, a large amount of preclinical data has been generated, demonstrating that RT can affect both the adaptive and innate immune responses (Rückert et al., 2021a). As a consequence, combinations of radio-immunotherapy are expanding and generating a lot of interest (Shevtsov et al., 2019). The adaptive immune system represents an attractive target for anti-cancer therapy as illustrated by the large amount of data generated with inhibitors of CTLA-4 (cytotoxic T-lymphocyte-associated protein 4) or targeting the immunosuppressive interaction between PD-L1 (Programmed death-ligand 1) and PD-1 (Programmed cell death protein 1), two ways to improve tumor control trough T cell activation. Associations of anti-CTLA4 with RT were among the first immunoradiotherapy combinations tested, which gave promising results such as the induction of systemic immune responses (Formenti et al., 2018). Moreover, PD-L1 expression is increased after RT (Deng et al., 2014), giving a strong rationale to the combination of RT with anti-PD-1/PD-L1, which has been largely tested in preclinical settings and then translated into clinical trials (Antonia et al., 2018; Shevtsov et al., 2019).

In addition to the widely studied effects of ionizing radiation (IR) on the adaptive immune response, radiotherapy also has a strong impact on tumor innate immune cell populations including natural killer (NK) cells (Patin et al., 2022; Walle et al., 2022) and myeloid cells as macrophages, monocytes, dendritic cells and neutrophils (Gómez et al., 2020; Schernberg et al., 2017). IR can promote the antitumor activity of myeloid cells in several ways: IR activates dendritic cells through the induction of immunogenic cell death and the release of "damage-associated molecular patterns" (DAMPs) (Wennerberg et al., 2017) and through the activation of the cGAS-STING pathway (Galluzzi et al., 2018). Moreover, it has been shown that IR modulates the phenotype of tumor-associated macrophages towards pro-immunogenic behaviors (Klug et al., 2013). Radiation can promote the recruitment of inflammatory cells, as $Ly6C^{high}$ monocytes (Mondini et al., 2019) and neutrophils (Takeshima et al., 2016), into the tumor micro environment (TME), but can also attract immunosuppressive cells (Kalbasi et al., 2017; Liang et al., 2017; Mondini et al., 2019).

Differently from subcutaneous tumor models, in orthotopic models, tumors or tumor cells are either implanted or injected into the target organ. This has the advantage to more closely resemble the natural tumor microenvironment of the equivalent tumor in human, making them more suitable than subcutaneous models to study the effects of anticancer therapies, especially when the role of the immune response is prominent. Accordingly, we and others have shown a different response of orthotopic *vs* subcutaneous tumors to the same treatment (Tran Chau et al., 2020; Zhao et al., 2017).

Here, we provide a detailed protocol to analyze by flow cytometry the myeloid cell populations in head and neck tumors orthotopically engrafted in syngeneic mice, and to evaluate their modulations induced by RT. Given the complexity and deeply heterogeneous composition of the myeloid compartment, the scope of this manuscript is to provide a basic protocol that may serve as a backbone to characterize the main myeloid populations. The flow cytometry panel here proposed could be adapted to more deeply characterize specific myeloid cell subsets and phenotypes, for instance by adding antibodies to detect specific markers. Moreover, the same method here presented, can be employed to study tumor-infiltrating myeloid cells from a variety of other mouse tumor models.

2. Materials:

Common disposables

- TC CLEARLINE culture flask 75 cm2 sterile CLEARLINE filter cap (#2515508, Dutscher) (see Note 1)
- Falcon conical bottom tube clarified PP 50 mL (#2515101, Dutscher)
- Insulin syringes, steriles, 0.3mL (#324826, BD Micro-Fine)
- Cell strainer 40µm Nylon (352340, Falcon)
- 70µm Cup filcons, sterile (#340634, BD Biosciences)
- Cluster tubes, individual, bulk 1.2mL polypropylene, non-sterile (#2048667, Corning, Fisher Scientific)
- Microplate, 96 walls (#209004, Porvair Science)

Common reagents

- RPMI 1640 W/GLUTAMAX-I (#61870044, Life Technologies)
- Foetal calf serum (#CVFSV00-01, Eurobio Scientific)
- Sodium Pyruvate 100mM (100X), (#11360-039, Life Technologies)
- Penicillin Streptomycin (#15140-122, Life Technologies)
- Minimum Essential Medium Non-Essential Amino Acids (100X) (11140-035, Life Technologies)
- Hepes Buffer Oslution (1M), (#15630056, Life Technologies)
- Trypsin-EDTA (0.05%), phenol red (#25300054, Life Technologies)
- PBS DULBECCO'S W/O CA MG (1X) (#14190169, Life Technologies)
- Trypan Blue solution 100mL (#T8154-100ML, SigmaAldrich)
- Isoflurane (#029405, Henry Schein)
- Beetle Luciferin, potassium salt. (E1602, Promega)
- Horizon Brilliant Stain Buffer Plus (#566385, BD Bioscience)
- CD16/32 (clone 93, from BioLegend)
- Nonfluorescent 10µm polybead® carboxylate microspheres suspension (Polysciences, Niles, IL, USA)
- DNAse 1 (#07469, Stem Cell)
- Collagenase Type IV (#17104-019, Gibco Life Technologies)
- Tumor dissociation kit (#130-096-730, Miltenyi Biotec)

Common equipment

- IVIS In Vivo Imaging System (Perkin Elmer)
- Varian Medical Systems 200kV irradiator
- ThermoMixer C (Eppendorf)
- LSR Fortessa II (BD)

3. Cell culture:

1. Firefly luciferase-expressing TC1/Luc cells, generated by the HPV16 E6/E7 and c-H-ras retroviral transduction of lung epithelial cells of C57BL/6 origin, were provided by T.C. Wu (Johns Hopkins Medical Institutions). Cells are cultured in 10mL of RPMI-1640 supplemented with 10% fetal bovine serum, 1% sodium pyruvate, 1% nonessential amino acids, 1% HEPES buffer and 1% penicillin/streptomycin antibiotics (complete culture medium) and maintained at 37°C in 5% CO2.
2. When reaching 80-90% confluence, remove the culture medium by aspiration, rinse with 3mL PBS and add 3mL 0.25% trypsin/EDTA solutions (75cm² flask). After 1-3 minutes and a complete detachment of the cell monolayer, add 9mL pre-warmed complete culture medium to the cell suspension to inactivate trypsin.
3. Centrifuge the cell suspension at 270g during 5 minutes at room temperature, remove the supernatant and resuspend the cell pellet in complete culture medium.
4. To maintain cell culture, use 10-20% of the cell suspension in the new 75cm² flasks containing 12mL complete culture medium (see Note 2).

4. Oral tumor implantation:

1. Six-eight mice can be included in each experimental group (two groups: one non-irradiated, one irradiated). For an experiment involving two groups each of six mice, culture TC1/Luc cells in two 75cm² flaks to obtain approximately 20 million cells (see Notes 3,4).
2. Remove the culture medium by aspiration, rinse with 3mL PBS and add 3mL 0.25% trypsin/EDTA solution. After 1-3 minutes and complete detachment of the cell monolayer, add 9mL pre-warmed complete culture medium to the cell suspension to inactivate the trypsin/EDTA (see Notes 5,6).
3. Centrifuge the cell suspension at 270g during 5 minutes and 4°C, remove the supernatant and resuspend the cell pellet in 10ml PBS (see Note 7).
4. Count cells in the presence of the viability dye trypan blue (see Notes 8,9,10,11).
5. Centrifuge the cell suspension at 270g during 5 minutes and 4°C, remove the supernatant and resuspend the cell pellet in PBS to obtain a concentration of 10^7 living cells/mL.
6. Anesthetize mice using an isoflurane gas chamber for 5 minutes. Then place one mouse at a time into a mask, which diffuses isoflurane gas to prevent the mouse from waking up during cell injection (see Notes 12,12).
7. Inject 50µL of cell suspension (containing $0.5x10^6$cells) at submucosal sites on the right inner lips of C57BL/6 mice (see Note 14).

5. In vivo imaging:

1. Six-seven days after tumor cells injection, monitor tumor signal using an in vivo imaging system (see Note 15).

2. Mice receive luciferin by intraperitoneal injection at 150mg/kg. Place mice in an anesthesia chamber that diffuses isoflurane gas (see Note 16).
3. After 10 minutes, mice are placed in the chamber of the imaging system to acquire the tumor bioluminescent signal (see Notes 17,18).
4. Signal quantification is performed and expressed as total light flux, in photons/second (see Notes 19,20).
5. Randomize mice in two groups according to their tumor signal
   Group 1: mock-irradiated
   Group 2: irradiated

6. Irradiation:

1. Perform a local irradiation to the head and neck region of the mice 7 days after tumor inoculation (**Fig. 1**). Mice are irradiated at the selected dose in a single fraction (see Notes 21,22).
2. Mock-irradiated mice are used as control.

7. Flow cytometry analysis:

1. Three days post irradiation, euthanize mice and collect tumors (see Note 23). Immediately put the tumors in ice-cold PBS (see Note 24).
2. Weight each tumor (see Note 25).
3. Cut tumors in small fragments using a scalpel (see Note 26).
4. Tumors are digested in RPMI or DMEM medium supplemented with collagenase IV and DNAse I for 30 minutes at 37°C in a shaker (see Notes 27,28).
5. During the incubation, prepare the fluorescent conjugated antibody mix (see Table 1 and Note 29)
6. Place a 40µm cell strainer onto an opened 50mL tube; put the dissociated tumor suspension into the cell strainer. Use the blunt end of a 2 or 5mL syringe to gently press the dissociated tumor through the cell strainer. Rinse the strainer with 5mL PBS to elute residual cells from the strainer.
7. Remove the strainer, close the tube and centrifuge it at 450g for 5 minutes in a pre-cooled centrifuge at 4°C. Remove the supernatant by decanting.
8. Resuspend the pellet with 1mL ice-cold PBS and transfer 100µL in a 96-wells plate (see Note 30).
9. Centrifuge the plate containing the samples at 450g during 5 minutes at 4°C and remove the supernatant by decanting.
10. Resuspend the pellet with 40µL anti-CD16/32 (Fc Block) and incubate 10 minutes at 4°C (see Note 31).
11. Add the antibody mix (10µL of mix, **Table 1**) to the wells for 25 minutes at 4°C in the dark (see Notes 32, 33).
12. Add 100µl of PBS, centrifuge the plate at 450g during 5 minutes at 4°C and decant the supernatant. Add 200µL of Flow Cytometry (FC) buffer. Resuspend the cell

pellet and transfer to microtubes containg each 10,000 of nonfluorescent 10μm polybead® carboxylate microspheres (see Notes 34, 35, 36).

13. Acquire data for each sample on a LSR Fortessa II (see Note 37).
14. Perform compensation for each fluorophore according to the instrument procedure.
15. Perform the gating strategy depicted in **Fig. 2**. (see Notes 38, 39).

Fluorescent-conjugate antibody	Dilution factor	Clone	Supplier
CD11b - BUV395	1/400	MI/70	BD
Ly6G - BV450	1/200	1A8	BioLegend
PD-L1 (CD274) - BV650	1/100	MIH5	BD
Siglec F - PETR	1/100	E50-2440	BD
Ly6C - APCCy7	1/100	AL-21	BD
IA/IE – BV510	1/200	2G9	BD
CD64 - PECy7	1/200	X54-5/71	BioLegend
CD11c - BV605	1/100	N418	BioLegend
CD103 - BV711	1/100	2E7	BD
CD45 - PCPCy5.5	1/200	30F11	BD

Table 1: Antibody mix to analyze myeloid cells in murine tumor samples.

8. Concluding remarks:

Fluorescence-activated flow cytometry is one of the most widely used technologies in immunology. It allows the rapid multiparametric analysis of cells on a cell-by-cell basis, and the widespread availability of flow cytometers capable of measuring more than ten parameters simultaneously (Perfetto et al., 2004) has much contributed to the improvement of our understanding of the multifaceted and dynamic landscape of the tumor immune environment. Flow cytometry has been widely used to analyze the immune populations following different antitumor treatments, including radiotherapy, in particular with a focus on the tumor and peripheral blood lymphoid compartment (Araya and Goldszmid, 2020; Donaubauer et al., 2019). On the other hand, it is now well known that radiotherapy also strongly affects myeloid cell populations. The protocol here described allows the identification and quantitative analysis of the main myeloid populations present in murine tumors. The panel presented in **Table 1** could be adapted to specific needs, for instance by adding antibodies to detect specific targets present at the cell membrane of myeloid cells. Examplesare the use of fluorescent-conjugated antibodies directed against PD-1, which would allow evaluating the levels of the receptor in the different immune populations, or against CD206 and CD80 to evaluate macrophage phenotype. When modifying the antibody panel, careful attention has to be put in the selection of the fluorescent conjugates, in order to avoid overlapping signals with the other detection antibodies. A much more detailed characterization of the tumor immune populations, including the detection of sub-populations and the information concerning the activation state of the cells, could be obtained using more advanced techniques as mass or spectral flow cytometry, which allow the use of multicolor panels with more than 40 parameters (Bonilla et al., 2020; Simoni et al., 2018). Nevertheless, the complexity of the set-up and the analysis of the data from such techniques, as well as the considerably increased time needed to acquire each sample, make conventional flow cytometry still the most widely used approach in immunology.

The oral tumor model here described was developed as a murine surrogate for human papillomavirus (HPV)-positive head and neck cancer, as the TC1/Luc cells express the proteins E6 and E7 from the oncogenic HPV16, and has been used by us and others in cancer research (Hamon et al., 2022; Mondini et al., 2015, 2019; Sandoval et al., 2013). The main caveat of this model is that TC1/Luc cells, despite being epithelial, were obtained by immortalizing primary lung cells of C57BL/6 mouse. The same procedure here described can be used to establish and analyze other head and neck models, e.g. the SCC VII orthotopic model in syngeneic C3H/HeN mice, which has been widely used as a model for research on head and neck carcinomas. This model has been described as being representative of the tumor microenvironment of head and neck squamous cell carcinomas (Brand et al., 2020). Moreover, the flow cytometry protocol here presented can be used to study the myeloid compartment of subcutaneous tumors, as the MC38 colorectal model (Meziani et al., 2020).

Radiation therapy, in particular in combination with immunotherapy, has the potential to induce systemic immune responses that can lead to the shrinking or disappearance of distant, non-irradiated tumour lesions, a phenomenon known as the abscopal effect (Brix et al., 2017). It is thus of interest to monitor the immune compartment of the local (irradiated) and abscopal (non-irradiated) tumours, which can significantly differ (Rückert et al., 2021b). The flow cytometry protocol here proposed can be applied to study the myeloid compartment of different murine models suited to analyse abscopal responses (Rodriguez-Ruiz et al., 2020).

More generally, the protocol here described can be used to analyze myeloid cells from a variety of murine tumors models, and could serve as a solid basis to evaluate the modulations of the tumor myeloid compartment induced by ionizing radiation, which can be applied at different IR doses, energies, and fractionation schemes.

9. Notes:

1. For all common material and equipment, catalog numbers and providers are indicated as a reference, but equivalent products can be purchased from a variety of providers.
2. TC1/Luc cells have a fast proliferation rate. Cells can be plated at a low density and can be routinely passaged 1:10 to 1:15 according to their confluence.
3. Cells can also be routinely maintained in supports other than 75cm² flasks, including 150 and 300cm² flasks. Larger flasks can be used to obtain the quantity of cells needed for *in vivo* injections.
4. Indicatively, when the monolayer reaches 80% confluence, a 75cm² flask of TC1/Luc cells contain 10-12x10^6 cells.
5. The volume of PBS and trypsin have to be adapted according to the size of the flask.
6. TC1/Luc cells are very sensitive to trypsin/EDTA. Incubation with trypsin/EDTA for 3 minutes at room temperature is generally sufficient to completely detach the cells.
7. Excessive centrifugation speeds (>500g) should be avoided as they induce mechanical stress potentially associated with cytotoxicity.
8. Live cells can be detected using trypan blue. Trypan blue is an exclusion dye used to selectively stain dead tissues or cells, it is an azo dye. Trypan blue is also known as diamine blue and Niagara blue. Prepare a working solution with 0.2% of the dye in PBS. Then, filter the solution with a 0.45µm filter to remove potential aggregates of the dye.

9. Trypan blue solution can be stored at room temperature protected from light.
10. To count cells, best results can be obtained using an automatic counter.
11. It is possible to use manual counting methods, as by using e.g. Buerker or Malassez counting chambers.
12. If using a "high flow" anesthesia system, airflow can be set at 1 L/min with 2.5% of isoflurane gas. The percentage isoflurane should not exceed 3%.
13. During cell injection into the right inner lips, the tube containing the cell suspension has to be mixed by inversion before each injection, to ensure homogeneity of the cell suspension.
14. Volume of injection must not exceed 50µL.
15. Acquisition of the bioluminescent signal can be performed using an IVIS In Vivo Imaging System.
16. Luciferin working solution can be prepared in advance at 15mg/mL and used at 10ml per kg mouse body weight. Store solution at -80°C.
17. The waiting time for each mouse in the anesthesia chamber before imaging must be between 9 and 14 minutes, which correspond to the plateau phase of the bioluminescent reaction in this model.
18. Carefully place the mice in the imaging system on their left flank, in order to expose the tumors in the right inner lip towards the camera.
19. Signal quantification can be performed using the imaging system software, as the Living Image Software (Perkin Elmer).
20. Select the region of interest (ROI) corresponding to the tumor area. When performing the analysis, do not use radiance or other units that are expressed as per unit area.
21. Mice are constrained in plastic holders before irradiation to prevent mice from moving during the irradiation procedure.
22. Localized RT can be performed with a variety of small animal irradiation devices, including a 200kV Varian Medical Systems, or X-RAD 320 (Precision X-Ray Inc., North Branford, CT, USA) cabinet irradiators. Selective irradiation of the tumor area can be performed using a lead plate with an opening to protect other parts of the mouse body. Alternatively, image-guided irradiators dedicated to small animals can be used, as the SARRP (Xstrahl Inc., Suwanee, GA, USA) or the X-RAD SmART (Precision X-Ray Inc). Different irradiation doses can be used, e.g. 8Gy in a single fraction with a dose rate of 1.08Gy/min using the Varian irradiator.
23. Euthanasia and subsequent analyses can be performed at different time points to evaluate the dynamics of the modulation of the response. The time points may be adapted according to the radiation dose and to the tumor model used.
24. After tumor collection, keep the tumors in PBS in an ice bath to preserve the cells.
25. Tumors are weighted after collection to allow normalization for the number of cells per mg of tissue. It is important to dry each tumor into a paper towel before weighting, not to affect the weight.
26. Before the dissociation, tumors have to be cut in small fragments to facilitate their subsequent enzymatic digestion.
27. Tumor tissues are dissociated into cells suspension using the enzymatic degradation of the extracellular matrix by collagenase IV (1 mg/mL) and using DNAse I (0.05 mg/mL) to reduce sample viscosity by degradation of the DNA. Place on a heat block at 37 °C for 30 min with shaking (e.g. 1500 rpm in a Thermomixer Eppendorf).
28. The tumor dissociation kit from Miltenyi Biotec can be also used. Prepare enzyme mix by adding 2.35mL of RPMI 1640 or DMEM, 100µL of Enzyme D, 50µL of Enzyme R, and 12.5µL of Enzyme A into a tube.

29. Prepare the mix by diluting each antibody indicated in Table 1 in the Horizon Brilliant Stain Buffer. Prepare a total 10µL mix for each sample, with an additional 20µL to have sufficient volume for all the samples. The Horizon Brilliant Stain Buffer is designed for the use with antibodies conjugated with BD Horizon Brilliant fluorescent polymer dyes, but it is compatible with the use of other fluorescent staining reagents, such as Alexa Fluor dye. It is possible to use flow cytometry buffer rather than Brilliant Stain Buffer.
30. Volumes indicated are for initial tumor fragments of around 300mg. Volumes can be adapted according to the tumor weight.
31. Fc receptors are found on monocytes, macrophages, dendritic cells and B cells and they bind antibodies via their constant Fc domain rather than the antigen specific Fab domain. This type of binding can lead to false positives signals and affect the data. In order to prevent the binding of the fluorescent conjugated antibodies, Fc blocking reagents have been developed and, when used before a staining protocol, they ensure saturation of Fc receptors, allowing that only the binding of the fluorescent conjugated antibodies to their antigens is observed. CD16/32 is used at 1/100.
32. A viability dye (a fluorescent dye that permeates the cells with compromised membranes, and that is non-permeant to live cells, e.g. the Zombie UV™ dye from BioLegend) may be included in the staining protocol to obtain precise information concerning the viability of the analyzed cells.
33. The CD11c and CD11b antibodies used in the proposed panel are highly specific for $CD45^+$ cells. Nevertheless, CD45 antibodies (as CD45-PCPcy5.5 clone 30F11 from BD) may be added to the antibody mix.
34. During last centrifugation, add 10µl of nonfluorescent 10µm polybead® carboxylate microspheres suspension, containing 10000 beads, to polypropylene cluster tubes 1.2mL from Corning.
35. Calculation of absolute cell numbers present in each gated population, for each sample, can be performed thanks to the addition of carboxylate microspheres. The following formula is used: number of cells = number of acquired cells in the gate of interest x 10000 / number of acquired beads (corresponding to the number of events in the population 1 in Fig. 2). The number of cells obtained for each sample can be normalized to the weight of tumor tissue, and expressed as absolute number of cells/mg. If needed, results can be also expressed as % of the parent population (not taking into account the results calculated with the beads).
36. Mircotubes can be used rather than flow cytometry tubes because it is easier to transfer the content of the 96 well-plates into microtubes.
37. Other flow cytometers capable of acquiring >10 channels can be used.
38. If using a viability dye, first gate on live cells starting from the gated population in Fig. 2B.
39. If using CD45 antibodies, first select $CD45^+$ cells from the gated population in Fig. 2B. If a viability dye is also used, gate on the $CD45^+$ cells from the live cells gated as in Note 38.

Acknowledgments

The authors received financial support from INSERM, SIRIC SOCRATE, Canceropole IdF, Fondation ARC pour la recherche sur le cancer (Projet Fondation ARC and ARC SIGN'IT), Institut National du Cancer (INCa 2018-1-PL BIO-06-1) and Fondation pour la Recherche Médicale (FRM DIC20161236437).

Disclosures

The authors declare grants from Roche Genentech, Servier, AstraZeneca, Merck Serono, Bristol-Myers Squibb, Boehringer Ingelheim, Eli Lilly and MSD, outside the submitted work. E.D. declares personal fees from Roche Genentech, AstraZeneca, MSD, AMGEN, Accuray and Boehringer Ingelheim outside the submitted work. E.D. declares shared patents with NH-Theraguix and Clevexel.

References

Antonia, S.J., Villegas, A., Daniel, D., Vicente, D., Murakami, S., Hui, R., Kurata, T., Chiappori, A., Lee, K.H., de Wit, M., et al. (2018). Overall Survival with Durvalumab after Chemoradiotherapy in Stage III NSCLC. N. Engl. J. Med. *379*, 2342–2350. https://doi.org/10.1056/NEJMoa1809697.

Araya, R.E., and Goldszmid, R.S. (2020). Characterization of the tumor immune infiltrate by multiparametric flow cytometry and unbiased high-dimensional data analysis. Methods Enzymol. *632*, 309–337. https://doi.org/10.1016/bs.mie.2019.11.012.

Baskar, R., Lee, K.A., Yeo, R., and Yeoh, K.-W. (2012). Cancer and Radiation Therapy: Current Advances and Future Directions. Int. J. Med. Sci. *9*, 193–199. https://doi.org/10.7150/ijms.3635.

Baumann, M., Ebert, N., Kurth, I., Bacchus, C., and Overgaard, J. (2020). What will radiation oncology look like in 2050? A look at a changing professional landscape in Europe and beyond. Mol. Oncol. *14*, 1577–1585. https://doi.org/10.1002/1878-0261.12731.

Bonilla, D.L., Reinin, G., and Chua, E. (2020). Full Spectrum Flow Cytometry as a Powerful Technology for Cancer Immunotherapy Research. Front. Mol. Biosci. *7*, 612801. https://doi.org/10.3389/fmolb.2020.612801.

Brand, M., Laban, S., Theodoraki, M.-N., Doescher, J., Hoffmann, T.K., Schuler, P.J., and Brunner, C. (2020). Characterization and Differentiation of the Tumor Microenvironment (TME) of Orthotopic and Subcutaneously Grown Head and Neck Squamous Cell Carcinoma (HNSCC) in Immunocompetent Mice. Int. J. Mol. Sci. *22*, 247. https://doi.org/10.3390/ijms22010247.

Brix, N., Tiefenthaller, A., Anders, H., Belka, C., and Lauber, K. (2017). Abscopal, immunological effects of radiotherapy: Narrowing the gap between clinical and preclinical experiences. Immunol. Rev. *280*, 249–279. https://doi.org/10.1111/imr.12573.

Deng, L., Liang, H., Burnette, B., Beckett, M., Darga, T., Weichselbaum, R.R., and Fu, Y.-X. (2014). Irradiation and anti-PD-L1 treatment synergistically promote antitumor immunity in mice. J. Clin. Invest. *124*, 687–695. https://doi.org/10.1172/JCI67313.

Donaubauer, A.-J., Rühle, P.F., Becker, I., Fietkau, R., Gaipl, U.S., and Frey, B. (2019). One-Tube Multicolor Flow Cytometry Assay (OTMA) for Comprehensive Immunophenotyping of Peripheral Blood. Methods Mol. Biol. Clifton NJ *1904*, 189–212. https://doi.org/10.1007/978-1-4939-8958-4_8.

Formenti, S.C., Rudqvist, N.-P., Golden, E., Cooper, B., Wennerberg, E., Lhuillier, C., Vanpouille-Box, C., Friedman, K., de Andrade, L.F., Wucherpfennig, K.W., et al. (2018). Radiotherapy induces responses of lung cancer to CTLA-4 blockade. Nat. Med. *24*, 1845–1851. https://doi.org/10.1038/s41591-018-0232-2.

Galluzzi, L., Vanpouille-Box, C., Bakhoum, S.F., and Demaria, S. (2018). SnapShot: CGAS-STING Signaling. Cell *173*, 276-276.e1. https://doi.org/10.1016/j.cell.2018.03.015.

Gómez, V., Mustapha, R., Ng, K., and Ng, T. (2020). Radiation therapy and the innate immune response: Clinical implications for immunotherapy approaches. Br. J. Clin. Pharmacol. *86*, 1726–1735. https://doi.org/10.1111/bcp.14351.

Hamon, P., Gerbé De Thoré, M., Classe, M., Signolle, N., Liu, W., Bawa, O., Meziani, L., Clémenson, C., Milliat, F., Deutsch, E., et al. (2022). TGFβ receptor inhibition unleashes interferon-β production by tumor-associated macrophages and enhances radiotherapy efficacy. J. Immunother. Cancer *10*, e003519. https://doi.org/10.1136/jitc-2021-003519.

Kalbasi, A., Komar, C., Tooker, G.M., Liu, M., Lee, J.W., Gladney, W.L., Ben-Josef, E., and Beatty, G.L. (2017). Tumor-Derived CCL2 Mediates Resistance to Radiotherapy in Pancreatic Ductal Adenocarcinoma. Clin. Cancer Res. Off. J. Am. Assoc. Cancer Res. *23*, 137–148. https://doi.org/10.1158/1078-0432.CCR-16-0870.

Klug, F., Prakash, H., Huber, P.E., Seibel, T., Bender, N., Halama, N., Pfirschke, C., Voss, R.H., Timke, C., Umansky, L., et al. (2013). Low-dose irradiation programs macrophage differentiation to an iNOS$^+$/M1 phenotype that orchestrates effective T cell immunotherapy. Cancer Cell *24*, 589–602. https://doi.org/10.1016/j.ccr.2013.09.014.

Liang, H., Deng, L., Hou, Y., Meng, X., Huang, X., Rao, E., Zheng, W., Mauceri, H., Mack, M., Xu, M., et al. (2017). Host STING-dependent MDSC mobilization drives extrinsic radiation resistance. Nat. Commun. *8*, 1736. https://doi.org/10.1038/s41467-017-01566-5.

Meziani, L., Gerbé de Thoré, M., Hamon, P., Bockel, S., Louzada, R.A., Clemenson, C., Corre, R., Liu, W., Dupuy, C., Mondini, M., et al. (2020). Dual oxidase 1 limits the IFNγ-associated antitumor effect of macrophages. J. Immunother. Cancer *8*, e000622. https://doi.org/10.1136/jitc-2020-000622.

Mondini, M., Nizard, M., Tran, T., Mauge, L., Loi, M., Clémenson, C., Dugue, D., Maroun, P., Louvet, E., Adam, J., et al. (2015). Synergy of Radiotherapy and a Cancer Vaccine for the Treatment of HPV-Associated Head and Neck Cancer. Mol. Cancer Ther. *14*, 1336–1345. https://doi.org/10.1158/1535-7163.MCT-14-1015.

Mondini, M., Loyher, P.-L., Hamon, P., Gerbé de Thoré, M., Laviron, M., Berthelot, K., Clémenson, C., Salomon, B.L., Combadière, C., Deutsch, E., et al. (2019). CCR2-Dependent Recruitment of Tregs and Monocytes Following Radiotherapy Is Associated with TNFα-Mediated Resistance. Cancer Immunol. Res. *7*, 376–387. https://doi.org/10.1158/2326-6066.CIR-18-0633.

Mondini, M., Levy, A., Meziani, L., Milliat, F., and Deutsch, E. (2020). Radiotherapy-immunotherapy combinations - perspectives and challenges. Mol. Oncol. *14*, 1529–1537. https://doi.org/10.1002/1878-0261.12658.

Patin, E.C., Dillon, M.T., Nenclares, P., Grove, L., Soliman, H., Leslie, I., Northcote, D., Bozhanova, G., Crespo-Rodriguez, E., Baldock, H., et al. (2022). Harnessing radiotherapy-induced NK-cell activity by combining DNA damage-response inhibition and immune checkpoint blockade. J. Immunother. Cancer *10*, e004306. https://doi.org/10.1136/jitc-2021-004306.

Perfetto, S.P., Chattopadhyay, P.K., and Roederer, M. (2004). Seventeen-colour flow cytometry: unravelling the immune system. Nat. Rev. Immunol. *4*, 648–655. https://doi.org/10.1038/nri1416.

Rodriguez-Ruiz, M.E., Yamazaki, T., Buqué, A., Bloy, N., Silva, V.A.O., Stafford, L., Sato, A., and Galluzzi, L. (2020). Monitoring abscopal responses to radiation in mice. Methods Enzymol. *635*, 111–125. https://doi.org/10.1016/bs.mie.2019.04.014.

Rückert, M., Flohr, A.-S., Hecht, M., and Gaipl, U.S. (2021a). Radiotherapy and the immune system: More than just immune suppression. Stem Cells Dayt. Ohio *39*, 1155–1165. https://doi.org/10.1002/stem.3391.

Rückert, M., Deloch, L., Frey, B., Schlücker, E., Fietkau, R., and Gaipl, U.S. (2021b). Combinations of Radiotherapy with Vaccination and Immune Checkpoint Inhibition Differently Affect Primary and Abscopal Tumor Growth and the Tumor Microenvironment. Cancers *13*, 714. https://doi.org/10.3390/cancers13040714.

Sandoval, F., Terme, M., Nizard, M., Badoual, C., Bureau, M.-F., Freyburger, L., Clement, O., Marcheteau, E., Gey, A., Fraisse, G., et al. (2013). Mucosal imprinting of vaccine-induced $CD8^+$ T cells is crucial to inhibit the growth of mucosal tumors. Sci. Transl. Med. *5*, 172ra20. https://doi.org/10.1126/scitranslmed.3004888.

Schernberg, A., Blanchard, P., Chargari, C., and Deutsch, E. (2017). Neutrophils, a candidate biomarker and target for radiation therapy? Acta Oncol. Stockh. Swed. *56*, 1522–1530. https://doi.org/10.1080/0284186X.2017.1348623.

Shevtsov, M., Sato, H., Multhoff, G., and Shibata, A. (2019). Novel Approaches to Improve the Efficacy of Immuno-Radiotherapy. Front. Oncol. *9*. https://doi.org/10.3389/fonc.2019.00156.

Simoni, Y., Chng, M.H.Y., Li, S., Fehlings, M., and Newell, E.W. (2018). Mass cytometry: a powerful tool for dissecting the immune landscape. Curr. Opin. Immunol. *51*, 187–196. https://doi.org/10.1016/j.coi.2018.03.023.

Takeshima, T., Pop, L.M., Laine, A., Iyengar, P., Vitetta, E.S., and Hannan, R. (2016). Key role for neutrophils in radiation-induced antitumor immune responses: Potentiation with G-CSF. Proc. Natl. Acad. Sci. *113*, 11300–11305. https://doi.org/10.1073/pnas.1613187113.

Tran Chau, V., Liu, W., Gerbé de Thoré, M., Meziani, L., Mondini, M., O'Connor, M.J., Deutsch, E., and Clémenson, C. (2020). Differential therapeutic effects of PARP and ATR inhibition combined with radiotherapy in the treatment of subcutaneous versus orthotopic lung tumour models. Br. J. Cancer *123*, 762–771. https://doi.org/10.1038/s41416-020-0931-6.

Walle, T., Kraske, J.A., Liao, B., Lenoir, B., Timke, C., von Bohlen Und Halbach, E., Tran, F., Griebel, P., Albrecht, D., Ahmed, A., et al. (2022). Radiotherapy orchestrates natural killer cell dependent antitumor immune responses through CXCL8. Sci. Adv. *8*, eabh4050. https://doi.org/10.1126/sciadv.abh4050.

Wennerberg, E., Vanpouille-Box, C., Bornstein, S., Yamazaki, T., Demaria, S., and Galluzzi, L. (2017). Immune recognition of irradiated cancer cells. Immunol. Rev. *280*, 220–230. https://doi.org/10.1111/imr.12568.

Zhao, X., Li, L., Starr, T.K., and Subramanian, S. (2017). Tumor location impacts immune response in mouse models of colon cancer. Oncotarget *8*, 54775–54787. https://doi.org/10.18632/oncotarget.18423.

Figure legends

Fig. 1 Treatment scheme for the head and neck orthotopic tumors. Mice are injected at day 0 with TC1/Luc cell in the right inner lips. Several days after inoculation, mice are randomized according to tumor bioluminescent signals. Mice are irradiated at 8Gy seven days post cell inoculation. At day 10, mice are euthanized to collect tumors for flow cytometry analysis.

Fig 2. Gating strategy used to analyze tumor myeloid cell populations. In order to properly identify the myeloid cell populations, cellular debris are excluded from the downstream analysis and nonfluorescent carboxylate microspheres (population 1) are identified using SSC-A and FSC-A (A). Then, gating on single cells (to exclude doublets) is done using FSC-W and FSC-H visualization (B). A gate is then placed to identify eosinophils using CD11b and Siglec F (C, population 2). $CD11b^{+}$ cells are then analyzed using Ly6C and Ly6G to identify neutrophils (D, population 3). $Ly6G^{-}$ cells population is characterized further to distinguish $Ly6C^{high}$ monocytes (E, population 4) from $Ly6C^{low}CD64^{+}$ macrophages (E, population 5). Finally, $Ly6C^{low}CD64^{-}$ population is analyzed for IA/IE and CD11c to discern type 2 conventional dendritic cells (F, population 6) and $Ly6c^{low}$ patrolling monocytes (F, population 7). The $CD11b^{-}$ population from panel C is analyzed for CD11c (G), then for CD103 and IA/IE levels to identify type 1 conventional dendritic cells (H, population 8).

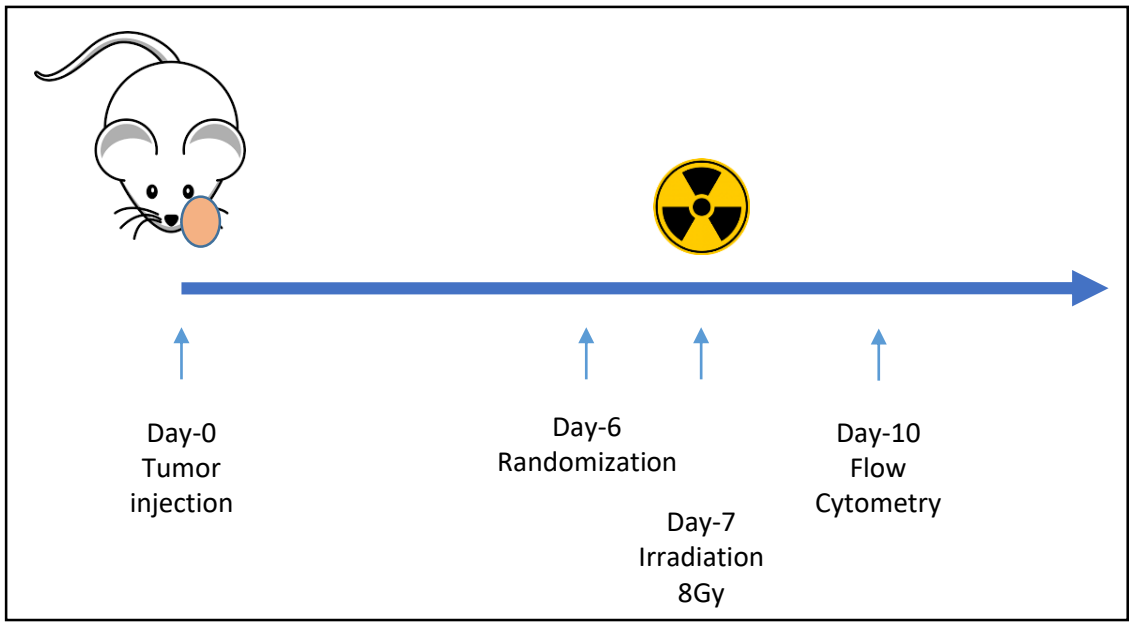
Day-0
Tumor
injection
Day-6
Randomization
Day-7
Irradiation
8Gy
Day-10
Flow
Cytometry

Figure 1

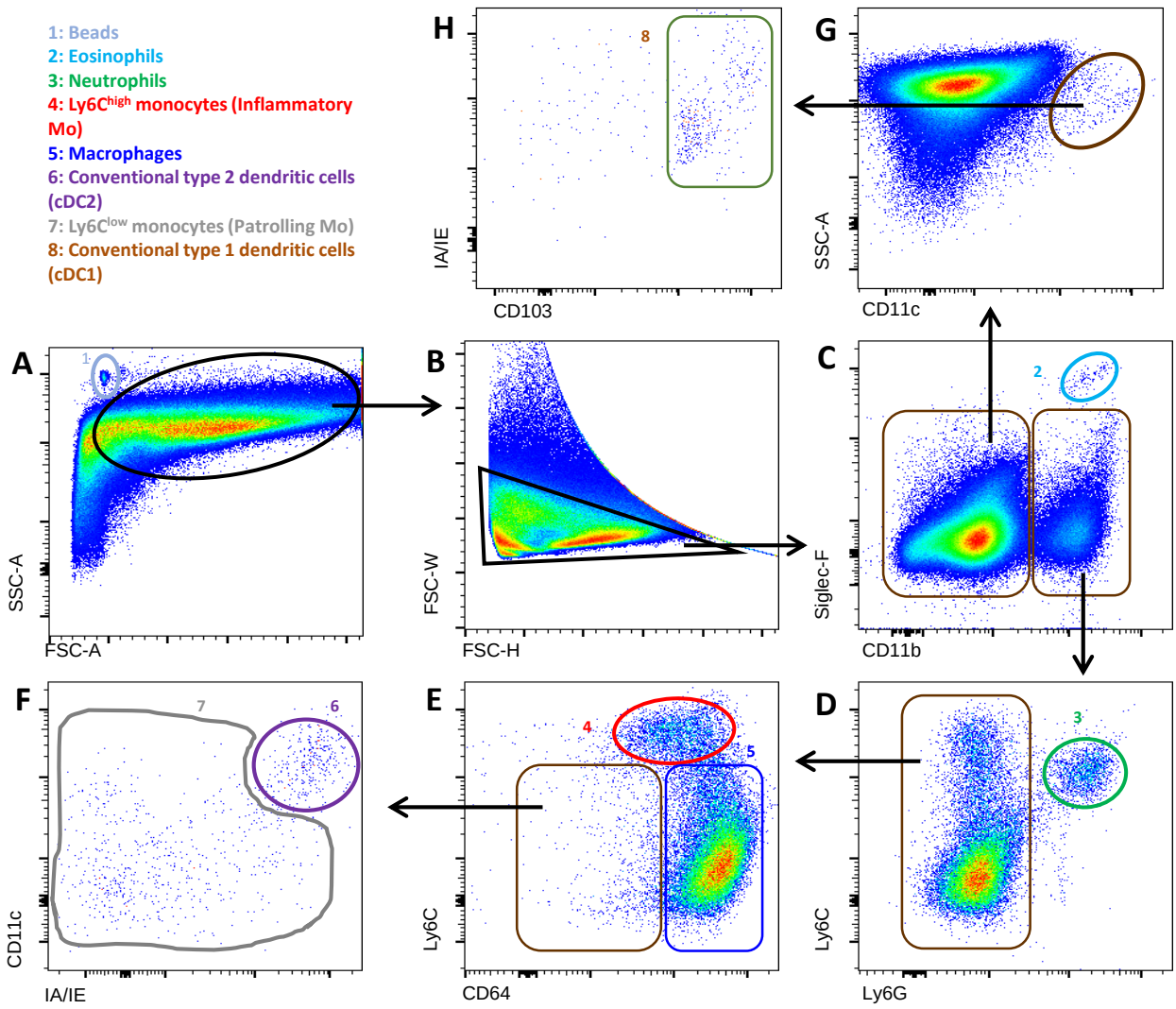
1: Beads
2: Eosinophils
3: Neutrophils
4: Ly6C^high monocytes (Inflammatory Mo)
5: Macrophages
6: Conventional type 2 dendritic cells (cDC2)
7: Ly6C^low monocytes (Patrolling Mo)
8: Conventional type 1 dendritic cells (cDC1)
A
SSC-A
FSC-A
B
FSC-W
FSC-H
C
Siglec-F
CD11b
D
Ly6C
Ly6G
E
Ly6C
CD64
F
CD11c
IA/IE
G
SSC-A
CD11c
H
IA/IE
CD103